Available online at www.sciencedirect.com
ScienceDirect
International Journal of Heat and Mass Transfer 50 (2007) 2132–2138
International Journal of HEAT and MASS TRANSFER
www.elsevier.com/locate/ijhmt

Constructal H-shaped cavities according to Bejan's theory

C. Biserni [a,*], L.A.O. Rocha [b], G. Stanescu [c], E. Lorenzini [a]

[a] Dipartimento di Ingegneria Energetica, Nucleare e del Controllo Ambientale, Università degli Studi di Bologna, Viale Risorgimento 2, 40136 Bologna, Italy
[b] Departamento de Física, Fundação Universidade Federal de Rio Grande, Av. Itália, Km 8, CP-474, Rio Grande, RS 96201-900, Brazil
[c] Departamento de Engenharia Mecânica, Universidade Federal do Paraná, Rua XV de Novembro 1299, Curitiba, PR 80060-000, Brazil

Received 29 September 2006
Available online 2 January 2007

Abstract

In this paper, we use Bejan's Constructal theory to optimize the geometry of a H-shaped cavity that intrudes into a solid conducting wall. The objective is to minimize the global thermal resistance between the solid and the cavity. Internal heat generation is distributed uniformly throughout the solid wall. The cavity surface is isothermal, while the solid wall has adiabatic conditions on the outer surface. The total volume and the volume of the H-shaped cavity are fixed, while the geometry of the H-shaped cavity is free to vary. Numerical results show that the optimal H-shaped configuration performs better than an optimal T-shaped cavity. The performance of the optimal H-shaped cavity is also superior to the performance of optimal rectangular and C-shaped cavities, which may be regarded as "elemental" configurations. Each of the optimized cavities, C-shaped, T-shaped and H-shaped, performs better when it penetrates the solid completely: this means that the geometrical complexity must evolve in order for the global flow system performance to improve.

Keywords: Constructal theory; Evolution of configuration; Geometry optimization; Morphing

1. Introduction

This paper documents numerically the fundamental relation between the maximization of global performance and the morphing architecture of a flow system. The morphing configuration is a H-shaped cavity that intrudes into a solid conducting wall. This work is an extension of the constructal method presented in [1,2], where we showed that the flow geometry is malleable, and it is deduced from a principle of global performance maximization subject to global constraints. Design is discovered (in the sense of Bejan's Constructal theory [3,4]), as the result of a "permanent struggle for better and better global system performance under global constraints".

The heat transfer literature has demonstrated how the principle of generating flow geometry works. Recent treatises on this subject [5,6] recount the evolution of cooling techniques for compact and miniaturized packages of electronics. The objective of the design is to install in a given volume as much circuitry as possible, i.e. as much heat generation rate as possible. The basic global constraint is that the package must fit into a given volume. The highest temperature, i.e. the hot spot, must not exceed a specified value: this makes the highest allowable temperature an ulterior global constraint.

Constructal theory is a hierarchical (telescopic) way of thinking that accounts for organization, complexity and diversity in nature, engineering and management. In Ref. [7], for example, it has been extended to economics. The principle of cost minimization (maximum flow access) in the transport of goods between a point and an area has been investigated in order to anticipate the dendritic pattern of transport routes that cover the area, and the shapes and numbers of the interstitial areas of the dendrite. Ref. [8] documents the fundamentals of the methods of exergy analysis and entropy generation minimization and the generation of flow architecture. Designed porous media and other interdisciplinary applications of the Constructal theory are reported in Refs. [9–11].

* Corresponding author. Tel.: +39 05120 93292; fax: +39 05120 93296.
E-mail address: cesare.biserni@mail.ing.unibo.it (C. Biserni).

0017-9310/$ - see front matter © 2006 Elsevier Ltd. All rights reserved.
doi:10.1016/j.ijheatmasstransfer.2006.11.006

Nomenclature

A	area, $A = HL$, m^2
H	height, m
H_0	thickness of the cavity tip, m
H_1	thickness of the vertical intrusion of the construct, m
H_2	stem thickness of the cavity, m
j	mesh index
k	solid thermal conductivity, W m^{-1} K^{-1}
L	length, m
L_0	half- length of the cavity tip, m
L_1	half- length of the vertical intrusion of the construct, m
L_2	stem length of the cavity, m
q'''	heat generation rate per unit volume, W m^{-3}
T	temperature, K
V	volume, m^3
V_0	cavity volume, m^3
W	width, m
x,y	cartesian coordinates, m

Greek symbol

ϕ	volume fraction occupied by the rectangular territory defined by the H-shaped structure

Superscript

(~)	dimensionless variables, Eqs. (5)–(7)

Subscripts

max	maximum
min	minimum
ref	reference

In this paper, we consider the constructal design in its original engineering sense, by focusing on the optimization of the architecture of an open cavity formed by a H-shaped intrusion. Open cavities are the regions formed between adjacent fins and they may represent essential promoters of nucleate boiling: see, for example, the Vapotron effect [12–14] that occurs as a consequence of the thermal interaction between a non-isothermal finned surface and a fluid locally subjected to a transient change of phase. In this paper, we consider the morphing and optimization of the H-shaped cavity in the most fundamental sense, without application to a particular device or field.

According to constructal theory, in the pursuit of maximal global performance the cavity shape is free to change subject to volume constraints. The global performance indicator is the overall thermal resistance between the volume of the entire system (cavity and solid) and the surroundings. For simplicity and clarity, we consider two-dimensional bodies with variable geometric aspect ratios, the rectangular solid and the H-shaped intrusion. Finally, in order to draw a comparison, a T-shaped cavity and a rectangular cavity are also optimized and evaluated.

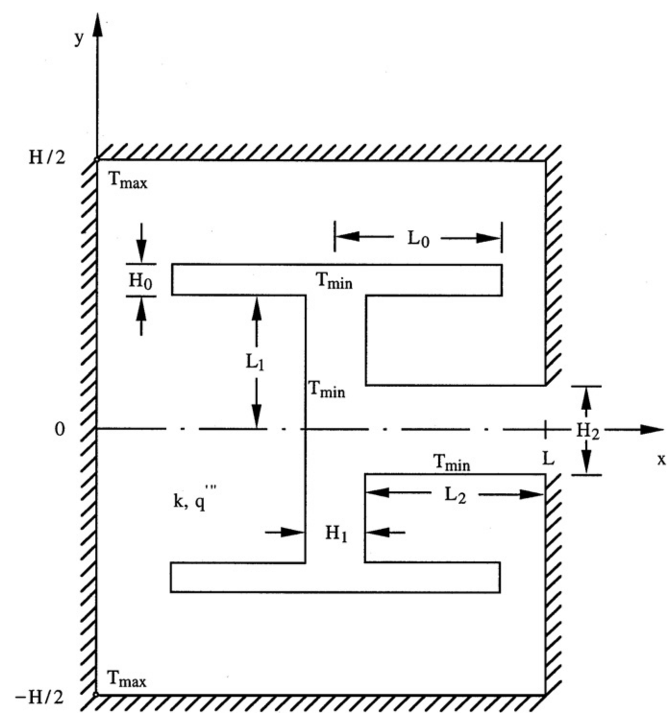

Fig. 1. Isothermal H-shaped intrusion into a two-dimensional conducting body with uniform heat generation.

2. H-shaped construct: numerical formulation and results

Consider the two-dimensional H-shaped conducting body shown in Fig. 1. The external dimensions (H,L) vary. The third dimension, W, is perpendicular to the plane of the figure. The total volume occupied by this body is fixed,

$$V = HLW. \tag{1}$$

Alternatively, the area $A = HL$ is fixed, because the configuration is two-dimensional. The dimensions of the cavity (H_0, L_0, H_1, L_1, H_2, L_2) also vary. The cavity volume is fixed,

$$V_0 = (4H_0L_0 + 2H_1L_1 + H_2L_2)W. \tag{2}$$

This second constraint may be replaced by the statement that the volume fraction occupied by the cavity is fixed,

$$\phi = \frac{V_0}{V} = \frac{4H_0L_0 + 2H_1L_1 + H_2L_2}{HL}. \tag{3}$$

The solid is isotropic with the constant thermal conductivity k. It generates heat uniformly at the volumetric rate q''' [W/m^3]. The outer surfaces of the heat generating body are perfectly insulated. The generated heat current ($q'''A$) is removed by cooling the wall of the cavity. The cavity wall temperature is maintained at T_{min}. Temperatures in the solid are higher than T_{min}. The hot spot of temperature T_{max} occurs at one or more points in the solid.

An important thermal design constraint is the requirement that temperatures must not exceed a certain level. This makes the hot spot temperature T_{max} a constraint. The location of T_{max} is not a constraint. The design calls for installing a maximum of heat generation rate in the fixed volume, which corresponds to packing the most electronics into a device of fixed size. In the present problem statement, this design objective is represented by the maximization of the global thermal conductance $q'''A/(T_{max} - T_{min})$, or by the minimization of the global thermal resistance $(T_{max} - T_{min})/(q'''A)$.

The numerical optimization of geometry consisted of simulating the temperature field in a large number of configurations, calculating the global thermal resistance for each configuration, and selecting the configuration with the smallest global resistance. Symmetry allowed us to perform calculations in only half of the domain, $y \geqslant 0$. The conduction equation for the solid region is

$$\frac{\partial^2 \widetilde{T}}{\partial \tilde{x}^2} + \frac{\partial^2 \widetilde{T}}{\partial \tilde{y}^2} + 1 = 0, \tag{4}$$

where the dimensionless variables are

$$\widetilde{T} = \frac{T - T_{min}}{q'''A/k}, \tag{5}$$

$$(\tilde{x}, \tilde{y}, \widetilde{H}, \widetilde{L}, \widetilde{H}_0, \widetilde{L}_0, \widetilde{H}_1, \widetilde{L}_1, \widetilde{H}_2, \widetilde{L}_2) = \frac{(x, y, H, L, H_0, L_0, H_1, L_1, H_2, L_2)}{A^{1/2}}. \tag{6}$$

The boundary conditions are indicated in Fig. 1. The maximal dimensionless excess temperature, $\widetilde{T}_{max}$, is also the dimensionless global thermal resistance of the construct,

$$\widetilde{T}_{max} = \frac{T_{max} - T_{min}}{q'''A/k}. \tag{7}$$

Eq. (4) was solved with a finite elements code based on triangular elements, developed in MATLAB environment and using the pde (partial-differential-equations) toolbox [15]. The domain is symmetric therefore, for the sake of simplicity, only half of the domain was used to perform the simulations. Fig. 2 shows the computational domain and the geometric details. The grid was non-uniform in both $\tilde{x}$ and $\tilde{y}$ directions, and varied for different geometries. The appropriate mesh size was determined by successive refinements, increasing the number of elements four times from one mesh size to the next, until the criterion $|(\widetilde{T}^j_{max} - \widetilde{T}^{j+1}_{max})/\widetilde{T}^j_{max}| < 5 \times 10^{-3}$ is satisfied. Here $\widetilde{T}^j_{max}$ represents the maximum temperature calculated using the current mesh size, and $\widetilde{T}^{j+1}_{max}$ corresponds to the maximum temperature using the next mesh, where the number of elements was increased by four times. Table 1 shows an example of how grid independence was achieved.

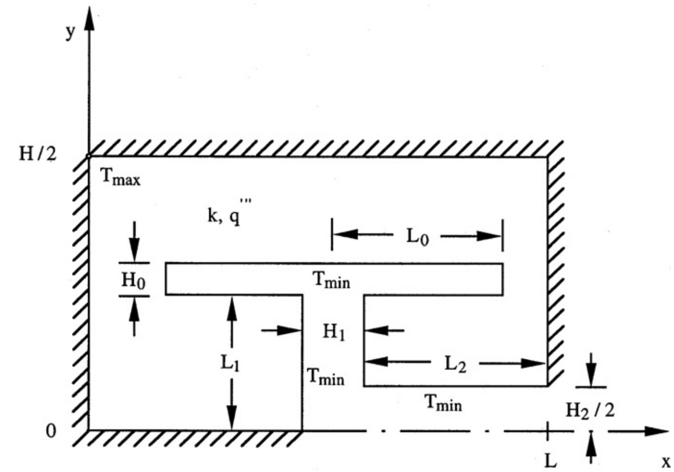

Fig. 2. Computational domain.

Table 1
Numerical tests showing the achievement of grid independence ($H/L = 1$, $\phi = 0.1$, $H_2/L_2 = 0.15$, $L1/L_2 = 0.6$, $L_0/L_2 = 0.6$, $H_1/L_2 = 0.75$, $H_0/H_2 = 1.0$)

Iteration	Elements	$\widetilde{T}_{max}$	$\lvert(\widetilde{T}^j_{max} - \widetilde{T}^{j+1}_{max})/\widetilde{T}^j_{max}\rvert$
1	174	0.089752	2.8×10^{-2}
2	696	0.092265	1.11×10^{-2}
3	2784	0.093291	4.4×10^{-3}
4	11,136	0.093699	–

Table 2
Comparison between the results obtained for an isothermal C-cavity in Ref. [1] and the present numerical work ($H/L = 1$, $\phi = 0.3$)

H_0/L_0	Ref. [1]	This work	Relative error
1.875	0.1873	0.1873	0
1.2	0.1436	0.1435	6.964×10^{-4}
0.8334	0.10865	0.1086	4.602×10^{-4}
0.4686	0.06574	0.0657	6.085×10^{-4}

The accuracy of the numerical method was also tested by reproducing with very good agreement the results presented by Ref. [1] for the isothermal C-cavity, which is an "elemental" rectangular open intrusion into a two-dimensional heat generating body. Table 2 shows several examples of this comparison.

3. Optimization of geometry

Fig. 1 reports the H-shaped cavity formed by a 'stem' intrusion ($L_2 \times H_2$) that branches into two elemental vertical intrusions ($L_1 \times H_1$), having at their tips two horizontal rectangles ($2L_0 \times H_0$). We solved the conduction problem in many configurations. The maximum temperature occurs in the upper-left corner of the domain. The optimization of the entire H-shaped intrusion forms the subject of this section. After having fixed $H/L = 1$, the H-shaped structure has five degrees of freedom that are represented by the ratios L_0/L_2, L_1/L_2, H_0/H_2, H_1/H_2 and H_2/L_2. Conse-

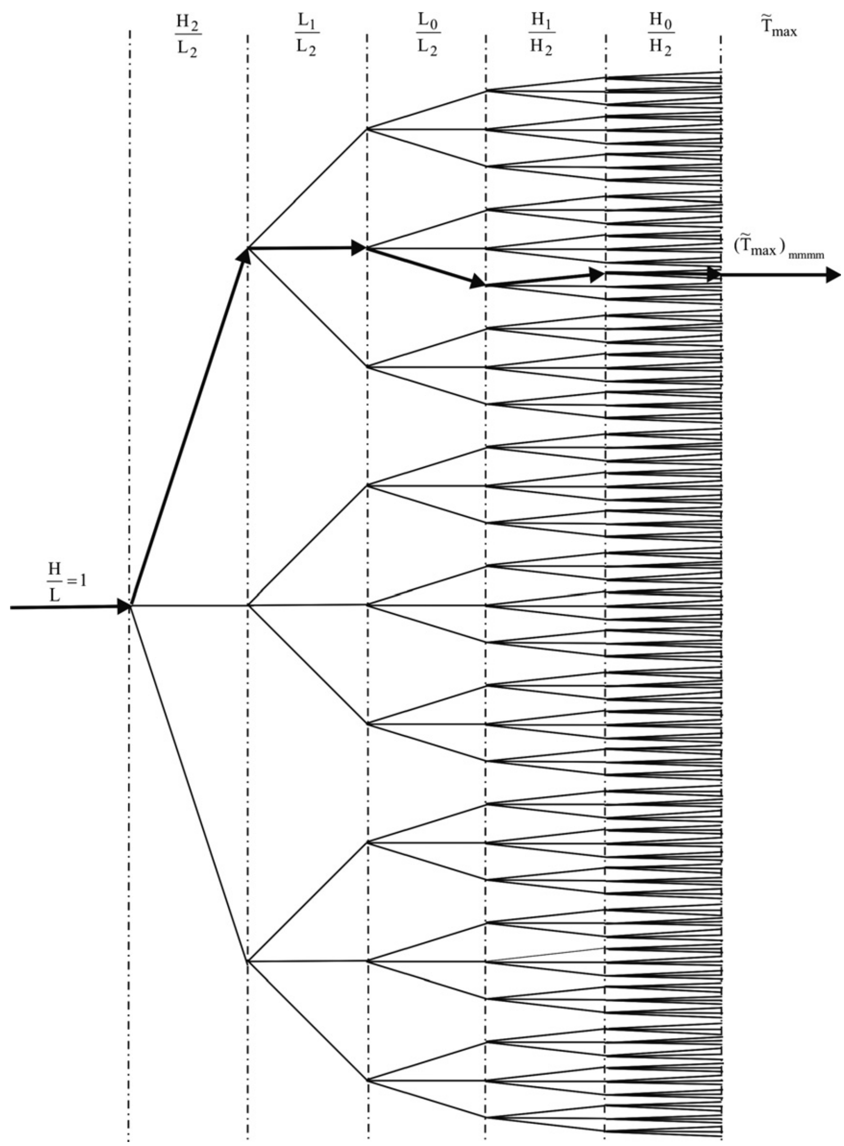

Fig. 3. Flow chart illustrating the optimization process.

quently, the optimization process has been divided into five steps as shown in Fig. 3.

In the first step, we optimized the geometry by varying the ratio H_0/H_2 and keeping fixed the remaining four geometric parameters. Fig. 4 shows that the thermal resistance can be minimized by selecting a particular shape of the cavity, namely the one with $H_0/H_2 = 0.16$. The optimal shape of the cavity is shown.

The procedure shown in Fig. 4 was repeated by optimizing the global thermal resistance with respect the degree of freedom H_1/H_2. Fig. 5 shows the minimized global thermal resistance, $(\widetilde{T}_{\max})_{\mathrm{m}}$, and its corresponding optimal ratio $(H_0/H_2)_{\mathrm{o}}$. The labels "m" and "o" mean that the H-cavity was optimized once, i.e., with respect to one degree of freedom. Fig. 5 also shows that there is a minimal value of $(\widetilde{T}_{\max})_{\mathrm{m}}$, called $(\widetilde{T}_{\max})_{\mathrm{mm}}$, and its corresponding optimized geometric parameters are called $(H_0/H_2)_{\mathrm{oo}}$ and $(H_1/H_2)_{\mathrm{o}}$.

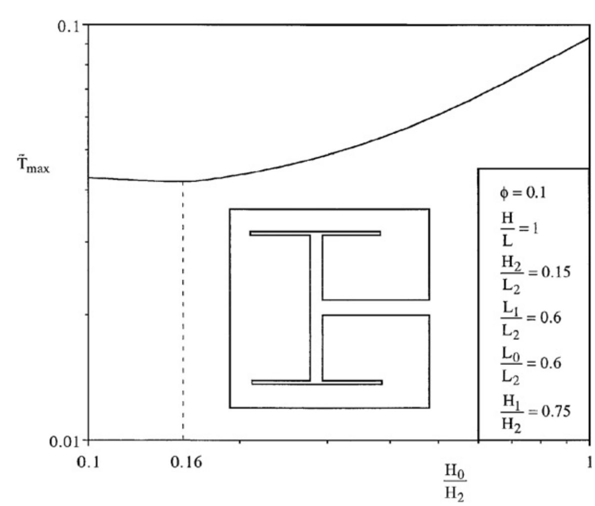

Fig. 4. First level of optimization: the minimization of the global thermal resistance as function of the ratio H_0/H_2.

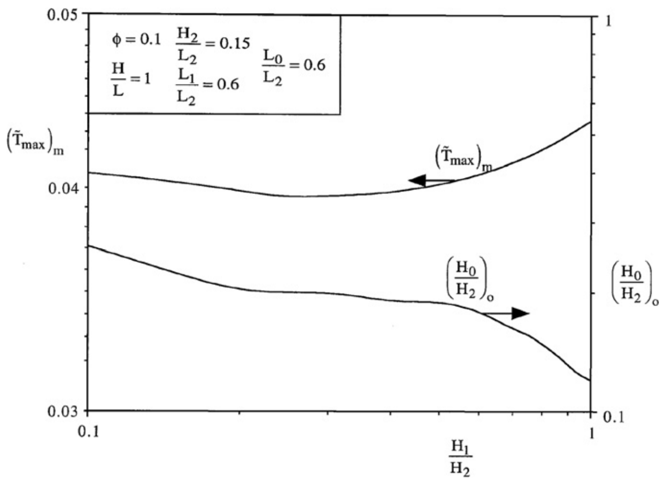

Fig. 5. Second level of optimization: the minimization of the global thermal resistance as function of the ratio H_1/H_2.

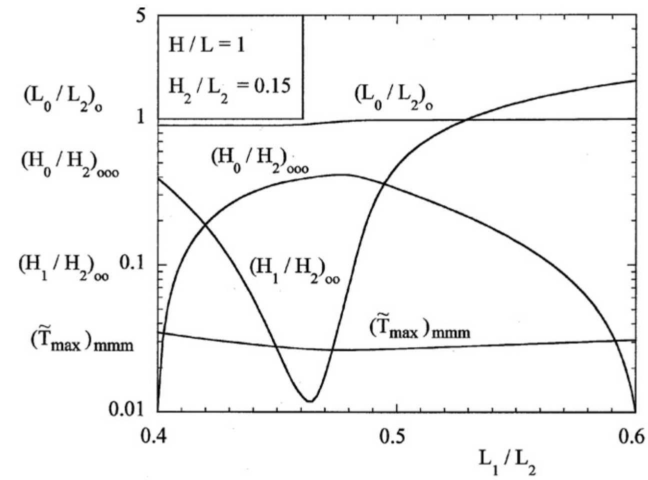

Fig. 7. Fourth level of optimization: the minimization of the global thermal resistance as function of the ratio L_1/L_2.

The next step in the optimizing process is to plot the optimized values obtained in simulations similar to the one performed in Fig. 5. Fig. 6 reports the optimal values for several values of the ratio L_0/L_2. The minimal global thermal resistance revealed in Fig. 6 is very pronounced and indicates that the ratio L_0/L_2 should also be examined in the design of the H-shaped cavity. The optimal corresponding shapes are also shown in Fig. 6.

Fig. 7 continues the search for better performance by varying the next degree of freedom: L_1/L_2. This fourth optimization completes the optimization for the ratio $H_2/L_2 = 0.15$, which was fixed at the start of the sequence shown in Figs. 4–6. Fig. 7 shows the minimal global thermal resistance optimized three times (in three nested loops) and its corresponding optimal shape parameters. This figure reports that the optimal ratio $(L_0/L_2)_o$ is approximately constant and very close to 1, indicating that this branch must occupy almost completely the length of the domain.

Fig. 8 presents the last step in the optimization process. This figure shows that the best structure is achieved when the ratio H_2/L_2 becomes as small as possible. The minimal global thermal resistance $(\widetilde{T}_{\max})_{\text{mmmm}}$ decreases, while the optimized ratios $(L_1/L_2)_{\text{o}}$ and $(L_0/L_2)_{\text{oo}}$ decrease and $(H_1/H_2)_{\text{ooo}}$ and $(H_0/H_2)_{\text{oooo}}$ increase. The results reported in Fig. 8 can be correlated with accuracy smaller than 4% by the expressions:

$$(\widetilde{T}_{\max})_{\text{mmmm}} = 0.0197\left(\frac{H_2}{L_2}\right)^{-0.126}\left(\frac{L_0}{L_2}\right)_{\text{oo}}^{0.266}\left(\frac{L_1}{L_2}\right)_{\text{o}}^{0.097} \times \left(\frac{H_0}{H_2}\right)_{\text{ooo}}^{-0.126}\left(\frac{H_1}{H_2}\right)_{\text{ooo}}^{-0.00433}, \tag{8}$$

$$\frac{H_2}{L_2} = 0.0484\left(\frac{H_0}{H_2}\right)_{\text{oooo}}^{-0.783}\left(\frac{H_1}{H_2}\right)_{\text{ooo}}^{-0.108}, \tag{9}$$

$$\left(\frac{L_0}{L_2}\right)_{\text{oo}} = 1.44\left(\frac{L_1}{L_2}\right)_{\text{o}}^{0.529}. \tag{10}$$

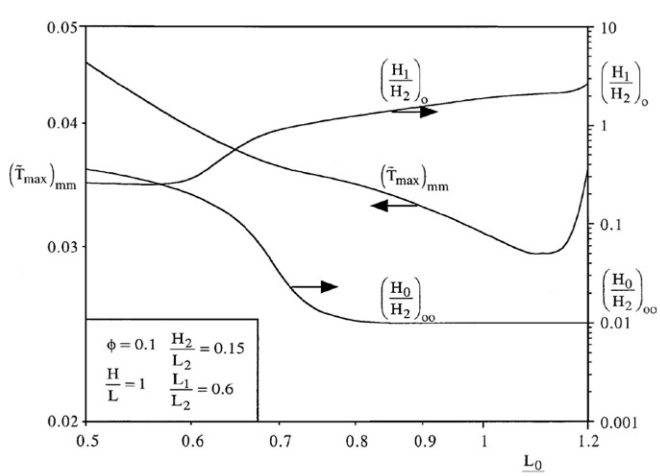

Fig. 6. Third level of optimization: the minimization of the global thermal resistance as function of the ratio L_0/L_2.

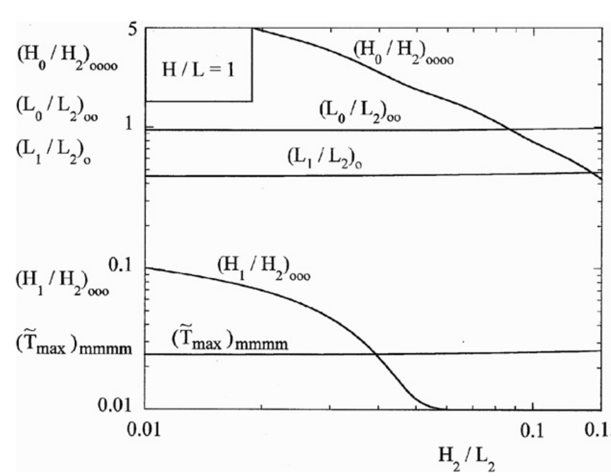

Fig. 8. Fifth level of optimization: the minimization of the global thermal resistance as function of the ratio H_2/L_2.

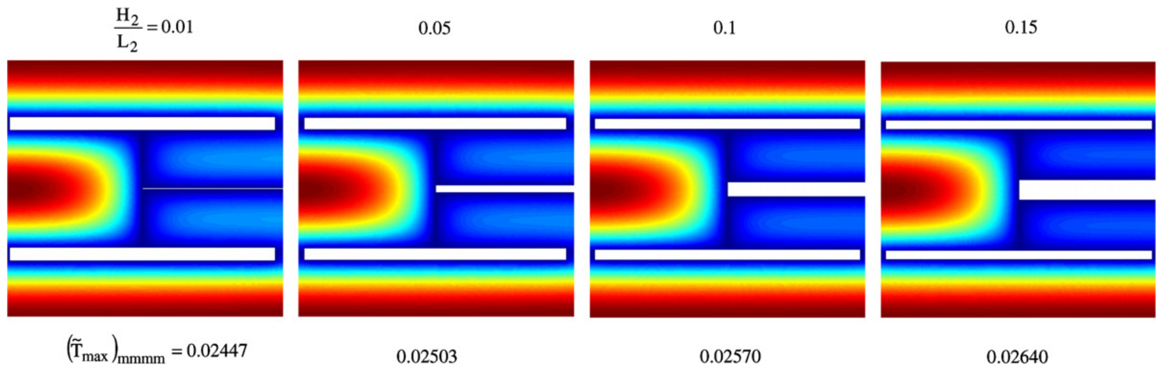

Fig. 9. The optimal configurations when $H/L = 1$.

Table 3
Comparison of the C-, T- and H-shaped cavities ($H/L = 1$, $\phi = 0.1$)

	$(\widetilde{T}_{\max})_{\text{opt}}$
C-shaped cavity	0.1008
T-shaped cavity	0.0710
H-shaped cavity	0.0245

In Fig. 9, we drew to scale the best H-cavities obtained by optimizing the global thermal resistance with respect to the five degrees of freedom.

According to Constructal theory the H-cavity shown in Fig. 1 can also be viewed as an example of a second construct, i.e. a construct resulted by the combination of two first constructs shaped as T cavities. Likewise, a T-cavity is an assembly of two elemental volumes, the C-cavities. Table 3 shows that the H-cavity, which is more complex, performs approximately four times better than the elemental cavity (C-shaped cavity). The H-shaped cavity is also almost three times more efficient than the T-shaped cavity under the same thermal conditions, uniform heat generation, volume fraction $\phi = 0.1$, and aspect ratio $H/L = 1$.

4. Conclusions

This work presented the optimization of a H-shaped cavity, which is a cavity formed by a stem intrusion ($L_2 \times H_2$) that branches into two elemental vertical intrusions ($L_1 \times H_1$), each continued by two smaller intrusions ($2L_0 \times H_0$). The global thermal resistance was minimized with respect to five degrees of freedom, while the total volume and the volume of the cavity were fixed. The geometry of the H-shaped cavity was free to vary. The results showed that the best architecture is achieved when the ratio H_2/L_2 becomes as small as possible. The behavior of the optimized configuration and performance was correlated by Eqs. (8)–(10) with accuracy better than 4%.

We showed that the H-shaped cavity can be construed as a second construct, i.e. a construct resulted by the combination of two first constructs, which are T-shaped. We also showed that the T-cavity is an assembly of two elemental volumes, which are C-shaped. We found that the H-shaped cavity performs approximately four times better than the elemental C cavity. The H cavity is almost three times more efficient than the T cavity. This comparison was done under the same thermal conditions, uniform heat generation and volume fraction occupied by the cavity.

In sum, the optimized sequence of configurations (C,T,H) shows that the geometrical complexity must evolve in order for the flow system to improve its global performance.

Acknowledgements

Dr. Cesare Biserni's work was supported by MIUR, Italy. Prof. Luiz Rocha's work was supported by FAPERGS, Porto Alegre, RS, Brasil.

References

[1] C. Biserni, L.A.O. Rocha, A. Bejan, Inverted fins: geometric optimisation of the intrusion into a conducting wall, Int. J. Heat Mass Transfer 47 (2004) 2577–2586.
[2] L.A.O. Rocha, E. Lorenzini, C. Biserni, Geometric optimization of shapes on the basis of Bejan's Constructal theory, Int. Commun. Heat Mass Transfer 32 (2005) 1281–1288.
[3] A. Bejan, Shape and Structure, from Engineering to Nature, Cambridge University Press, Cambridge, UK, 2000.
[4] A. Bejan, Advanced Engineering Thermodynamics, second ed., Wiley, New York, 1997, Chapter 13.
[5] S.P. Gadag, S.K. Patra, V. Ozguz, P. Marchand, S. Esner, Design and analysis: thermal emulator cubes for opto-electronic stacked processor, J. Electron. Packaging 124 (2002) 198–204.
[6] A. Bejan, Optimal internal structure of volumes cooled by single-phase forced and natural convection, J. Electron. Packaging 125 (2003) 200–207.
[7] A. Bejan, V. Badescu, A. De Vos, Constructal theory of economics, Appl. Energ. 67 (2000) 37–60.
[8] A. Bejan, Fundamentals of exergy analysis, entropy generation minimization, and the generation of flow architecture, Int. J. Energ. Res. 26 (2002) 545–565.
[9] A. Bejan, Simple methods for convection in porous media: scale analysis and the intersection of asymptotes, Int. J. Energ. Res. 27 (2003) 859–874.
[10] A. Bejan, Flows in environmental fluids and porous media, Int. J. Energ. Res. 27 (2003) 825–846.
[11] A. Bejan, I. Dincer, S. Lorente, A.F. Miguel, A.H. Reis, Porous and Complex Flow Structures in Modern Technologies, Springer-Verlag, New York, 2004.

[12] H.D. Falter, E. Thompson, Performance of hypervapotron beam-stopping elements at jet, Fusion Technol. 29 (1996) 584–594.
[13] C. Biserni, G. Lorenzini, Experimental tests on subcooled boiling heat transfer under forced convection conditions, J. Eng. Thermophys. 11 (2002) 73–81.
[14] G. Lorenzini, C. Biserni, A Vapotron effect application for electronic equipment cooling, J. Electron. Packaging 125 (2003) 475–479.
[15] MATLAB, User's Guide, Version 6.0.088, Release 12, 2000, The Mathworks, Inc.